Materials Science in Additive Manufacturing

REVIEW ARTICLE

Cold spray additive manufacturing of copper-based materials: Review and future directions

Vineeth Menon[1], Clodualdo Aranas Jr.[2]*, Gobinda Saha[1]

[1]Nanocomposites and Mechanics Laboratory, University of New Brunswick, Fredericton, Canada

[2]Alloy Design and Materials Testing Research Laboratory, University of New Brunswick, Fredericton, Canada

Abstract

The cold gas dynamic spray process is a manufacturing process strategically designed for coatings. The conditions for the deposition of materials to form coatings have evolved over several decades. Copper and copper-based cold spray coatings are an interesting field for investigation, as it has substantial commercial demand and acceptance. Several important works have already been performed in this regard that shows the immense popularity of its applications in power industries. Cold gas dynamic spray, being an economic process, can produce coatings with superior quality and low oxidation. In this paper, a particular focus has been given to copper-based cold spray coatings along with their deposition parameters. The various mechanical, electrical, corrosion, and tribological properties of these copper-based cold spray coatings are commendable and economically lucrative. A good amount of experimental data has also been included in this review article to provide comprehensive information and future scope of research about copper-based cold spray coatings.

Keywords: Cold spray; Copper-based alloys; Coatings

***Corresponding author:**
Clodualdo Aranas Jr.
(clod.aranas@unb.ca)

Citation: Menon V, Aranas Jr. C, Saha G, 2022, Cold spray additive manufacturing of copper-based materials: Review and future directions. *Mater Sci Add Manuf.* 1(2): 1-20.
https://doi.org/10.18063/msam.v1i2.12

Received: April 28, 2022

Accepted: June 8, 2022

Published Online: June 27, 2022

1. Introduction

Copper, having good ductility and exceptional thermal and electrical properties, has a great potential to be employed as coatings for different substrates according to their commercial acceptance in aerospace, automobile, power, and metallurgical industries. There are several coating processes to form copper-based coatings with various reinforcements, such as the cold gas dynamic spray process (CGDS), which is a prominent and essential additive manufacturing technique for research and industrial applications. The cold gas dynamic spray additive manufacturing technique has a wide commercial acceptance. This technique was first developed in the 1980s at the Institute of Theoretical and Applied Mechanics of the Siberian division of the Russian Academy of Science at Novosibirsk[1,2]. To date, the cold spray process technology is gaining a lot of attention from researchers for its exceptional capability of depositing powders onto the substrate without any high-temperature phase transformations or oxidation. The dense and adequately thick coatings having proper corrosion resistance and desirable mechanical properties make cold-sprayed coatings supreme. The CGDS is a low-temperature process that sprays powder particles onto a substrate; these

powder particles are accelerated with the help of carrier gas. Hence, the particles impact the substrate with high kinetic energy and form the coatings[3-5].

1.1. Production of metal powders

There are several methods to produce metal powders required for spraying purposes, additive manufacturing, and other fields. These methods include mechanical milling, atomization, chemical precipitation, and reduction. In the atomization process, the liquid metal alloy is continuously dispersed in the form of fine droplets due to the impact of the medium used for atomization. The different types of atomization processes are gas, water, plasma, and centrifugal atomization; plasma and gas atomization techniques are the most popularly used[6]. However, the spherical powders produced by such techniques have a low cold spray deposition efficiency compared to irregular-shaped powders. For this reason, mechanical milling remains a popular choice for creating powders for the cold spraying process[7].

1.2. Powder feedstock preparation for cold spraying

A prominent powder processing technique for processing the powder feedstock before the cold spraying is mechanical ball milling. In this process, the powder mixtures are subjected to high-energy collision by the impact of metallic balls, leading to two opposing mechanisms, and these mechanisms are cold welding and fracturing of the powder particles. A higher amount of ceramic reinforcements leads to more fracturing of powder particles; hence, smaller powder sizes can be achieved. Furthermore, these ball-milled powders are then cold sprayed with the help of a convergent-divergent nozzle and a carrier gas to increase the speed of powder particles to supersonic velocity[8]. The convergent-divergent nozzle has an inlet and outlet with a pressure difference existing between them. The gas flows in the convergent part of the nozzle at a subsonic speed and then accelerates to supersonic velocity in the divergent part of the nozzle. The parameters such as dimensions of the nozzle, type of the gas used, gas temperature, and pressure help determine the in-flight characteristics of the powder particles[7].

1.3. Role of surfactants in mechanical alloying

Mechanical treatment by ball milling is advantageous for the preparation of composite powders[9-13]. Mechanical alloying involves mixing different metals and forming an intimate powder mixture as a product. On the other hand, mechanical milling is a process of reducing the powder sizes with uniform chemical composition. These two processes take place due to the high-energy impact of the balls on the powder particles, resulting in cold welding and fracturing. As a result, the powder particles always have atomistic clean surfaces that might allow them to get combined, resulting in welding. However, with time, plastic deformation of powder particles also increases, leading to the fracture of particles. In this process, the powder particles may probably adhere to the vial and ball surfaces. Ductile particles are more prone to the cold welding process. The cold welding of ductile particles can be controlled either by altering the surface of these particles or by milling at cryogenic temperatures[14].

The altering of the surface of powder particles can be achieved using process control agent (PCA) or commonly referred to as surfactants. The surfactants get absorbed into the powder particle surfaces, as shown in Figure 1, which results in a decrease in cold welding and an increase in fracturing. This may be due to the decrease in surface energy of the newly formed surfaces of powder particles, which prevents them from cold welding. The use of surfactants in the milling of ductile powder particles increases powder yield.

The amount of surfactant used should be appropriate enough to cover the surfaces of the powder particles completely so as to serve as a deterrent to cold welding of the particles. Moreover, the quantity of surfactant required for the purpose of milling is dependent on: (i) The ductility of the powders to be milled, (ii) thermal as well as chemical cost ability of the PCA or surfactants, (iii) quantity of powder to be milled and its initial size, and (iv) duration of milling. For example, the amount of surfactant for ductile materials is higher than that of the brittle materials. Surfactants with a large molecular weight (like stearic acid) form monolayers by adsorption on powder particles. On

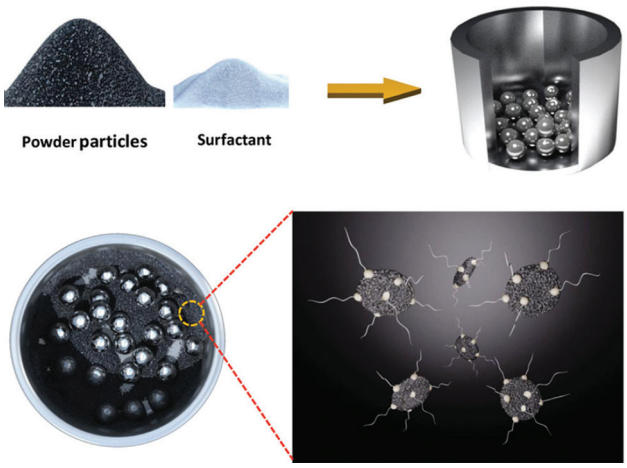

Figure 1. Surfactant added to the powders for ball milling. Surfactants get adsorbed to the surface of the powder particles preventing them from agglomeration[14]. (Reprinted from *Critical Reviews in Solid State and Materials Sciences*, 39(2), Nouri, A., and Wen, C, Surfactants in Mechanical Alloying/Milling: A Catch-22 Situation, 81 – 108, 2014, with permission from Taylor and Francis).

the other hand, methanol (with lower molecular weight) allows multilayer formations on the powder particles. The multilayer formation can reduce the cold welding of the powder particles while milling[14]. Kollo *et al.*[15] investigated that there was no sticking of aluminum silicon carbide powders on the milling tool when heptane was utilized instead of stearic acid as a surfactant. Some other factors governing the quantity of surfactant required for mechanical milling/alloying processes are speed of milling, milling temperature, and ball-to-powder ratio. These factors can greatly affect the adsorption of surfactants on the surface of the powder particles.

Lu and Zhang[16] demonstrated the effect of the amount of surfactants used during milling on the milling time. They reported that the aluminum-magnesium powder yield after milling with 4 wt.% stearic acid was much higher than the milling done with 1 wt.% stearic acid for the same milling time. Another critical observation by Shaw *et al.*[17] was the decrease in crystallite size with the increase in milling time. However, with the increase in the amount of surfactants, the actual crystallite size increases. They reported that powders milled for 4 h without any surfactant had the same crystallite size as that of powders milled for 8 h with 1 wt.% stearic acid and almost the same for powders milled for 16 h with 2 wt.% stearic acid. Furthermore, the hardness of powders is affected by the reaction of surfactants with powder particles. Kollo *et al.*[15] observed that when heptane was used as a surfactant, the hardness of powder particles was less compared to the case when stearic acid was used as a surfactant during milling. Therefore, the choice of surfactant and its amount to be used for milling have great significance in deciding the milling parameters before cold spraying the milled powders.

1.4. Cold spray process

Among additive manufacturing-based technologies, there are two distinct groups of techniques primarily divided based on their functional task, material types being handled, or the degree of complexity in their deposition process. These are powder based and non-powder based. In the non-powder feed method, such as wire arc AM or laser melt deposition wire, a wire feed is melted in a nozzle through plasma arc or laser. Whereas in the powder feed deposition method, the powder as feedstock is sprayed onto a substrate in a supersonic/transonic atmosphere to develop 3D coatings or freeform objects through self-consolidation. The technique thus works as a direct AM process in high productivity requirements.

The common denomination among the two groups is the requirement of a high thermal energy source, either in the form of laser, oxy-fuel combustion, flame spray, or detonation spray. Compared with these technologies, cold spray neither uses high temperature (e.g., selective laser melting or direct metal deposition) nor engages in complex chemical processes (e.g., electroplating). This makes cold spray the best fit for working with geometries of complex shapes and simultaneously accomplishing deposition without thickness limitation. According to ASTM F2792-12A standard, cold spray is a promising AM technology in the industry-scale manufacturing landscape. This standard is later replaced by ISO/ASTM 52900:2021.

In the cold spray process, the parameters that determine a successful deposition also include particle morphology shape, type of the material, and the standoff distance between substrate and nozzle. The gases used for cold spray are helium, nitrogen, and air[7]. Helium is costly and is helpful in cases where powder particles should reach high critical velocity required for highly dense coatings. Helium provides a good working temperature; however, nitrogen and air can cut the cost of the manufacture of coatings[18]. Nitrogen can also prevent oxidation of the coatings[7]. Furthermore, annealing treatments could be a good alternative to increase the denseness of the coatings instead of using a costly process gas[19].

The typical size range of the powder particles required for a successful cold spray should be less than 100 μm. The particles having a size larger than 100 μm may not get cold sprayed as they are difficult to get accelerated to supersonic velocity by the carrier gas. In general, for depositing composite powders, the spray conditions and parameters are typical, and they may not be the same as the parameters used for single-powder deposition. Before spraying, the different powders are mechanically milled together to make composite agglomerate. In a cermet powder feedstock, the metal powder particles act as a binder and help to ameliorate bonding. A combination of soft metal powders and hard ceramic powders can prevent damage to the hard ceramic particles and, hence, help in retaining the desired properties intended. This mechanical milling also enhances the deposition efficiency and forms thick coatings[7,20]. Figure 2 shows the parameters required to obtain a successful cold-sprayed coating.

1.5. The metal-ceramic interface bonding characteristics in the cold spray process

Combining ceramics and metals is difficult due to their different bonding characteristics. In ceramics, atoms have ionic and covalent bonds; on the other hand, metals are normally associated with metallic bonds. The flow of electrons is restricted in ceramics. Moreover, the stable ionic and covalent bonds in ceramics reduce surface interactions,

reducing adherence with metal. There is also a mismatch in the thermal expansion coefficient of metal and ceramic, which makes the bonding difficult and may also result in interfacial cracks. Cold spray is an excellent technique for making an effective metal-ceramic interface because it is a low-temperature process that avoids any melting of particles or phase transformations. The effectiveness of adherence between metal-ceramic interfaces produced by the cold spray technique can have a great effect on their mechanical and tribological properties[21].

The powder particles, having a velocity greater than the critical velocity, get deposited on the substrate. These powder particles with high supersonic velocity bombard the surface of a substrate and essentially perform the desired work of removing the oxide layer on the substrate, enhancing the bonding of coatings to the substrate in the presence of ceramic particles along with the metal particles, enhancing the bonding characteristics. The ceramic particles do not deform themselves, but they distort the ductile metal matrix and enhance the bonding. These ceramic particles may also break into fragments and, hence, get embedded in the metal matrix all around, which may eventually increase the hardness of the coatings. The cermet particles serve the following functions: (i) Cleaning the nozzle, (ii) activating the sprayed surface, and (iii) densifying the structure[3,22].

2. Pure copper cold spray coatings

Copper as an element specifically known for its exceptional electrical and thermal conductivities is greatly used for thermal and electrical applications commercially in various industries. Several studies have been conducted to explore the properties of pure copper and copper-based cold spray coatings to prove its superiority in terms of quality, sustainability, and economy as compared to other available methods for producing coatings.

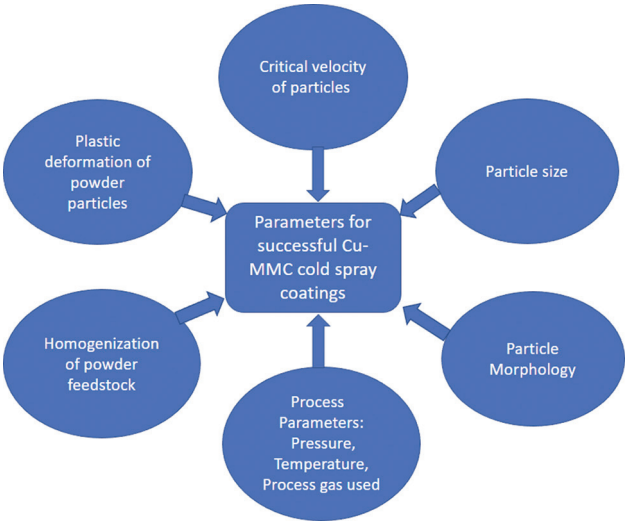

Figure 2. Parameters for successful Cu-MMC cold spray coatings.

Fukumoto *et al.*[23] reported the study of deposition behavior and efficiency of cold-sprayed copper coatings with respect to changes in substrate temperature, particle velocity, gas pressure, and gas temperature. The copper particles have mean sizes 5, 10, and 15 µm. According to their observations, the 5 µm copper particles produced an increase in particle velocity with an increase in gas pressure during the cold spraying process. However, the effect of gas temperature was not significant on particle velocity. The particle velocity was highest for 5 µm copper particles and lowest for 15 µm copper particles; this observation shows that particle velocity significantly varies with particle mean size. Moreover, higher copper particle velocity leads to better deposition efficiency.

In the same study, it was also reported that an increase in the temperature of the substrate could lead to improved deposition. This increase was even more pronounced when both pressures of the gas and substrate temperature were increased. Figure 3 shows the increase in deposition of copper particles with respect to the substrate temperature and pressure. This observation could be of good use in designing the parameters for cold spray deposition[23].

Borchers *et al.*[24] studied the deformation behavior of cold-sprayed copper coatings by focusing on various areas in the coating microstructures seen in the transmission electron microscopy micrographs (Figure 4). The regions marked as A, B, C, and D in the micrograph correspond to the copper particle-particle boundaries. Region "D" shows

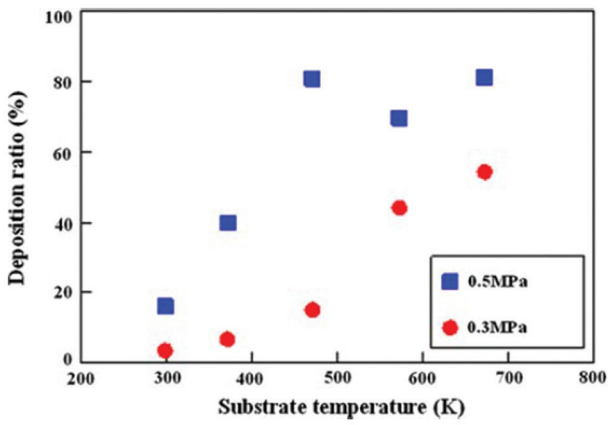

Figure 3. Deposition of copper particles with respect to substrate temperature and gas pressure[23]. (Reprinted from *Journal of Thermal Spray Technology*, 16, Fukumoto, M., Wada, H., Tanabe, K., Yamada, M., Yamaguchi, E., Niwa, A., Sugimoto, M., and Izawa, M., Effect of Substrate Temperature on Deposition Behavior of Copper Particles on Substrate Surfaces in the Cold Spray Process, 643-650-108, 2007, with permission from Springer Nature).

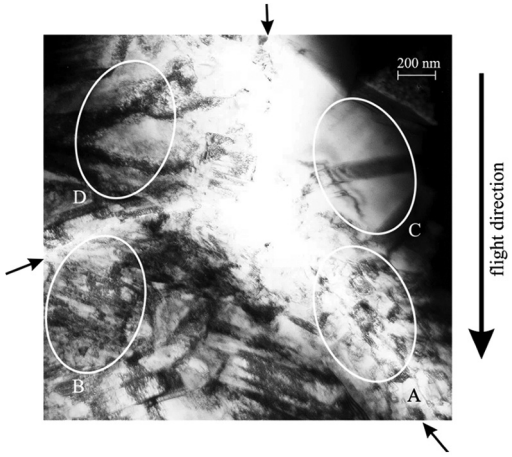

Figure 4. A particle-particle triple point of cold-sprayed copper coating is seen in this TEM micrograph[24]. (Reprinted from Materials Research Society Symposium – Proceedings, 674, Borchers, C., Stoltenhoff, T., Gärtner, F., Kreye, H. and Assadi, H., Deformation microstructure of cold gas sprayed coatings, P7.10.1-P.10.6, 2001, with permission from Springer Nature).

high dislocation density having dislocation arrangement in walls. The marked Region "B" displays aligned elongation of grains with high dislocation density. Then, Region "A" reveals the ultrafine grains with high dislocation density, specifically at the grain boundaries. Finally, Region "C" shows dislocation-free regions having deformation twins. The direction of flight of the particles has been marked on the micrograph along with three other directions showing the particle-particle interface.

Basically, particles can be seen making a triple point. Between Regions B and D, the particle-particle interface is 70°, and between Regions A and C, the particle-particle interface is 45°. As seen in the micrograph, there are particles impacting at different angles, according to which the local temperatures may also be different. This may give rise to the process of recrystallization, which can account for microstructural changes as compared to the initial powder feedstock. As discussed by Borchers *et al.*[24], Region C consisted of twins. This could be due to the high strain rate deformation and subsequent recrystallization during annealing caused by local temperature increase. Due to the extremely short cooling time of around 10^{-4} s, the fraction of coating that has recrystallized is very less. As far as the deformation in Regions A, B, and D is concerned, there could be several steps into which the whole recrystallization process can be divided; first, the formation of randomly distributed dislocations; second, the development of long dislocation cells due to dynamic recovery; and third, the elongated subgrains form, followed by the breaking up and formation of small equiaxed grains. In Region A, the rise in temperature is the highest because of the equiaxed grains visible in this region. However, in Region B, only the breaking up of elongated subgrains was visible, suggesting that the temperature increase was not too high as compared to the region A. Furthermore, in Region D, only dislocation cells were seen and not the subgrains, which shows that the temperature rise was even lesser as compared to the Region B as well as A.

Borchers *et al.*[24] also measured the resistivity of the copper coatings, which was identified to have values close to the resistivity of cold-rolled copper sheets. In their work, they suggested that the cold-sprayed coatings can acquire better electrical properties when compared to high-velocity oxygen fuel (HVOF)-fabricated copper coatings. The copper coatings produced by cold spray were very dense, consisting of good metallic bonding between the particles. Most importantly, the oxide formation was negligible in cold-sprayed copper coatings. However, the bond strength of HVOF copper coatings is higher than the bond strength of copper cold spray coatings.

3. Copper-based metal matrix composite cold spray coatings

The metal matrix composite coatings with copper as the base metal are of great commercial importance. Copper-based MMC coatings can be utilized in power industries, especially in the manufacturing of seam welding electrodes, electrical contacts, lead wires, and conductors for high-temperature electrical applications. These coatings can be produced through techniques such as HVOF and CGDS. The oxide formations and phase transformations in the HVOF coatings degrade the properties of the coatings. The CGDS process is currently being utilized in fabricating various copper-based MMC coatings. Several reinforcements such as SiC, CNT, AlN, graphene, alumina, MoS_2, WC, and TiB_2 have been employed to make successful cold spray coatings. Each reinforcement has characteristic properties; thus, they are selected accordingly to impart the same worthy properties in the copper metal matrix composite coatings. Several research projects have already been done in this area, proving the worth of such composite coatings, which are reviewed in the next section.

4. Recent investigations into copper-based MMC coatings

4.1. Copper-alumina cermet coatings

Several studies have been done on copper as a metallic matrix with ceramic reinforcement (also known as cermets). Recently, special attention has been given to ameliorating mechanical properties and wear resistance of various copper-based coatings using hard particles as

additives[25-27]. For example, Koivuluoto *et al.* successfully deposited copper + alumina coatings onto a substrate via cold spray process. Dendritic and spherical copper powders were mixed with 10 vol.%, 30 vol.%, and 50 vol.% of alumina. Then, its cold spraying characteristics were compared with that of the pure copper coatings made with dendritic and spherical copper powders. The thickness of the copper-alumina coatings increased with the increasing amount of alumina ceramic particles, mainly due to the hammering effect of alumina particles on the ductile copper matrix. The shot peening effect of the ceramic particles deforms the copper powders; thus, porosity decreases, which enhances the bonding characteristics. According to Koivuluoto *et al.*, the densest coatings obtained were for dendritic copper + 50 vol.% alumina and 10 vol.% alumina + spherical copper. Figures 5-8 show the field emission scanning electron microscopy (SEM) micrographs of these coatings. The reason for this, as reported, was that the dendritic copper particles have a higher surface area and are more prone to oxidation as compared to the spherical copper powders. Eventually, these dendritic copper powders require more deformation to achieve better metal-metal bonding and an effective dense coating. However, the Vickers hardness of copper + alumina coatings showed a constant rise with the increase in alumina particles for the coatings obtained. With both dendritic and spherical copper particles, the Vickers hardness for all the coatings obtained with spherical copper powders is higher (ranging between 106 Hv and 127 Hv) when compared to the coatings obtained with dendritic copper particles (ranging 83 – 103 Hv). The corrosion resistance of these coatings made with spherical copper powders + alumina was higher than the dendritic copper powder coatings. The spherical copper + alumina powder coatings were denser, as reported in the literature[28].

In another work, Phani *et al.*[29] successfully cold-sprayed nanocrystalline copper-alumina powders and studied the effect of heat treatments at the temperatures of 300°C, 600°C, and 950°C, and inferred that alumina particles were effective in stopping the grain growth, which is of immense value for commercial applications. Figure 9 shows the micrographs of the as-sprayed and heat-treated coatings. The variation in the grain size due to the heat treatments, as reported, was significantly less for copper-alumina coatings compared to pure copper coatings. The same trend was detected for microhardness, where nanocrystalline copper-alumina coatings had higher hardness than the pure copper coatings for all heat treatment temperatures. As reported, the copper-alumina

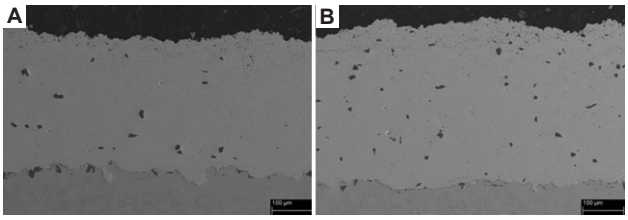

Figure 5. Field emission scanning electron microscopy micrographs of (A) dendritic copper + 10 vol.% Al_2O_3 and (B) dendritic copper + 30 vol.% coatings on steel substrate[28]. (Reprinted from *Journal of Thermal Spray Technology*, 19(5), Koivuluoto, H., and Vuoristo, P., Effect of Powder Type and Composition on Structure and Mechanical Properties of Cu + Al_2O_3 Coatings Prepared using Low-Pressure Cold Spray Process, 1081 – 1092, 2010, with permission from Springer Nature).

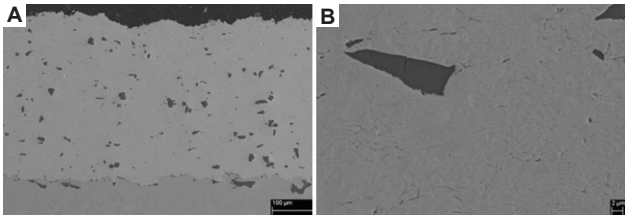

Figure 6. Field emission scanning electron microscopy micrographs of (A) dendritic copper + 50 vol.% Al_2O_3 coatings on steel substrate and its (B) detailed microstructure[28]. (Reprinted from *Journal of Thermal Spray Technology*, 19(5), Koivuluoto, H., and Vuoristo, P., Effect of Powder Type and Composition on Structure and Mechanical Properties of Cu + Al_2O_3 Coatings Prepared using Low-Pressure Cold Spray Process, 1081 – 1092, 2010, with permission from Springer Nature).

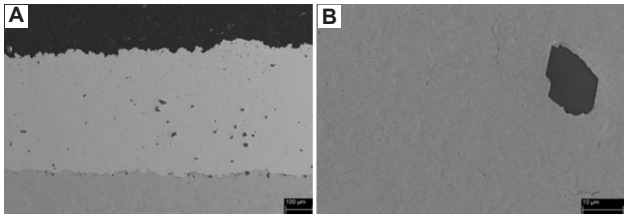

Figure 7. Field emission scanning electron microscopy micrographs of (A) spherical copper + 10 vol.% Al_2O_3 coatings on steel substrate and its (B) detailed microstructure[28]. (Reprinted from *Journal of Thermal Spray Technology*, 19(5), Koivuluoto, H., and Vuoristo, P., Effect of Powder Type and Composition on Structure and Mechanical Properties of Cu + Al_2O_3 Coatings Prepared using Low-Pressure Cold Spray Process, 1081 – 1092, 2010, with permission from Springer Nature).

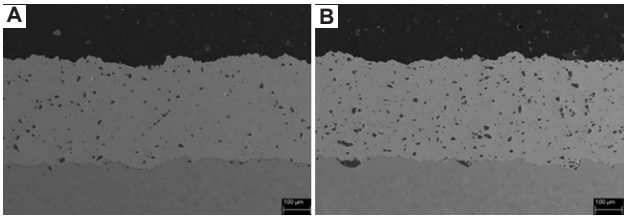

Figure 8. Field emission scanning electron microscopy micrographs of (a) spherical copper + 30 vol.% Al_2O_3 and (B) spherical copper + 50 vol.% coatings on steel substrate[28]. (Reprinted from *Journal of Thermal Spray Technology*, 19(5), Koivuluoto, H., and Vuoristo, P., Effect of Powder Type and Composition on Structure and Mechanical Properties of Cu + Al_2O_3 Coatings Prepared using Low-Pressure Cold Spray Process, 1081 – 1092, 2010, with permission from Springer Nature).

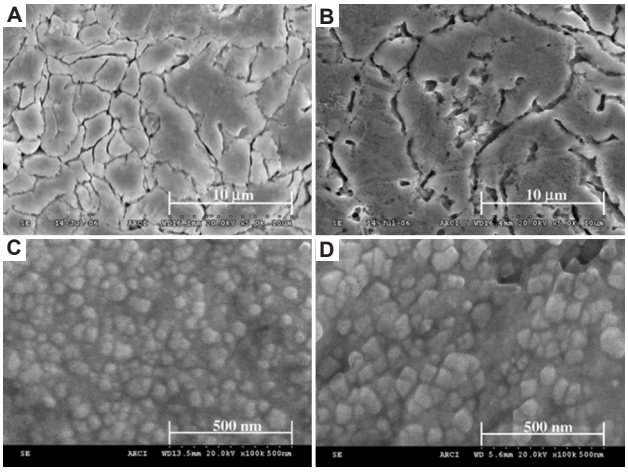

Figure 9. Microstructure of (A) copper coating (as-sprayed), (B) copper coating heat treated at 950°C, (C) copper-alumina coating (as sprayed), and (D) copper-alumina coating heat treated at 950°C[29]. (Reprinted from *Acta Materialia*, 55, Sudharshan Phani, P., Vishnukanthan, V., and Sundararajan, G., Effect of heat treatment on properties of cold-sprayed nanocrystalline copper-alumina coatings, 4741 – 4751, 2007, with permission from Elsevier).

coatings showed only a 9% reduction in hardness post-heat treatment at 950°C, whereas the pure cold-sprayed copper showed a 55% decrease in hardness, which gives nanocrystalline copper-alumina coatings an edge over coarse-grained copper coatings. The electrical conductivity of nanocrystalline copper-alumina coatings was reported to be around 20 – 25 MS/m, which is lesser than the conductivity of nanocrystalline copper coatings which had a reported value of around 50 MS/m. This electrical conductivity behavior of the coatings could be attributed to the presence of alumina ceramic particles[29].

In addition to the studies above, Winnicki *et al.*[30] studied the corrosion resistance of copper-alumina cold spray coatings with cyclic salt spray and Kesternich tests. As reported, even after 18 cycles of NaCl sprays on copper-alumina coatings, there was no significant corrosion, possibly because of the low amount of ceramic particles in the Cu + Al_2O_3 coating accounting to lesser weak metal ceramic interfaces allowing the chloride ions to penetrate in them, so there was no buckling in the coatings. However, for the Kesternich test performed in sulfur dioxide environment, there were some small cracks at the boundary between the substrate and the coatings. Furthermore, the electrical conductivity test performed on copper-alumina coatings also did not show a huge difference in electrical conductivity between as-sprayed copper-alumina coatings and the copper-alumina coatings after the two corrosion tests (salt spray and Kesternich tests). The electrical conductivity reported for as-sprayed copper-alumina coating was 62% IACS. However, interestingly, the drop in electrical conductivity of copper-alumina coatings was very less after the salt spray test and Kesternich test. Electrical conductivity values of 51% IACS and 58% IACS were measured for copper-alumina coatings after salt spray and Kesternich tests, respectively. According to the analysis, there were layers of $Cu_2Cl(OH)_3$ (paracetamite), which might also enhance corrosion resistance[30].

Chen *et al.*[31] prepared copper-alumina-graphite cold-sprayed coatings (for lubrication purposes) with 304 stainless steel plates as substrates. The feedstock powders prepared were pure copper, copper-alumina (10 wt.%), and copper-alumina (10 wt.%)-copper-coated graphite (5 wt.%, 10 wt.%, and 20 wt.%) powders. As reported, the pure copper coatings had around 365 µm thickness along with small pores. However, with the incorporation of 10 wt.% alumina, the number of pores was significantly reduced, possibly due to the hammering effect of alumina ceramic particles. The thickness of the coating also drastically improved to 859 µm. However, with the addition of copper-coated graphite, the thickness of coatings was reduced to 480, 400, and 562 µm for copper-alumina (10 wt.%)-copper-coated graphite (5 wt.%, 10 wt.%, and 20 wt.%) cold-sprayed coatings, respectively. Figure 10 shows SEM micrographs of Cu-based solid lubricating cold spray coatings.

As reported, among the hardness values of copper-based coatings, copper-alumina coatings had the highest Brinell hardness of 114.3 as compared to the pure copper coating with a Brinell hardness of 97.0 as well as with copper-alumina-copper-coated graphite coatings ranging around 107.3 – 88.2. There was a decrease in hardness with the increasing amount of copper-coated graphite in the copper-based LPCS solid lubricant coatings. The lamellas of copper in the copper-alumina-copper-coated graphite 5 wt.% are large with less plastic deformation. However, with the increase in copper-coated graphite content from 5 wt.% to 10 wt.% and further to 20 wt.%, the relative plastic deformation increased, which could be mainly due to the hammering effect and the relatively higher amount of alumina in copper-alumina (10 wt.%)-copper-coated graphite (10 wt.% and 20 wt.%)[31].

Dry sliding wear performance of copper-based solid lubrication coatings was also studied by Chen *et al.*[31]; they found that the pure copper coatings had a friction coefficient of 0.82 and the copper-alumina coatings had a friction coefficient of 0.94. With the incorporation of copper-coated graphite, the friction coefficient was reduced due to the increase in solid lubrication. The reported values of friction coefficients were 0.69, 0.29, and 0.34 for copper-alumina (10 wt.%)-copper-coated graphite (5 wt.%, 10 wt.%, and 20 wt.%) cold-

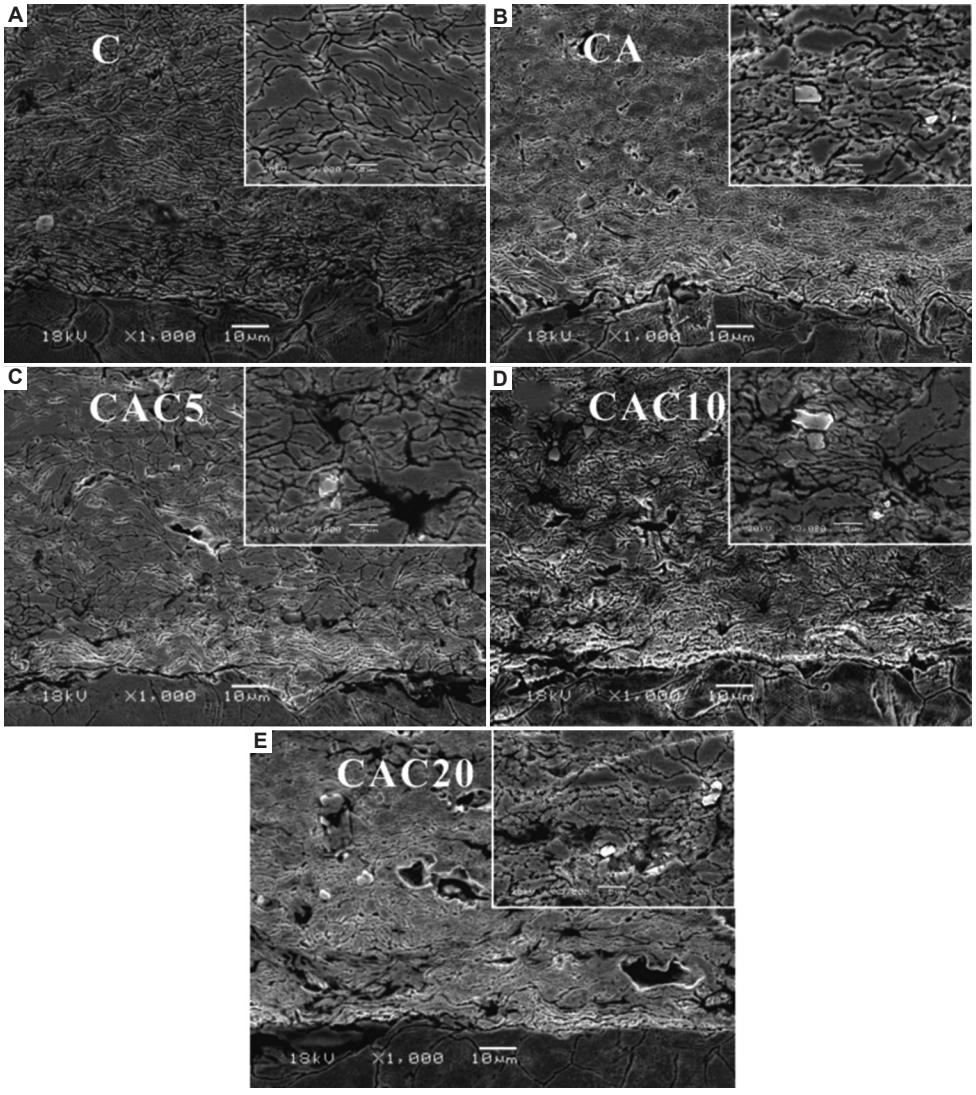

Figure 10. Scanning electron microscopy micrographs of Cu-based solid lubricating cold spray coatings: (A) Copper, (B) copper-alumina, (C) copper-alumina-copper-coated graphite 5 wt.%, (D) copper-alumina-copper-coated graphite 10 wt.%, and (E) copper-alumina-copper-coated graphite 20 wt.%[31]. (Reprinted from *Journal of Thermal Spray Technology*, 27(8), Chen, W., Yu, Y., Cheng, J., Wang, S., Zhu, S., Liu, W., and Yang, J., Microstructure, Mechanical Properties and Dry Sliding Wear Behavior of Cu-Al_2O_3-Graphite Solid-Lubricating Coatings Deposited by Low-Pressure Cold Spraying, 1652 – 1663, 2018, with permission from Springer Nature).

sprayed coatings, respectively. The wear rate of these copper-based coatings also improved with the addition of copper-coated graphite. The reported values were 2.53×10^{-4} mm^3/Nm, 2.18×10^{-4} mm^3/Nm, and 1.2×10^{-4} mm^3/Nm for copper-alumina (10 wt.%)-copper-coated graphite (5 wt.%, 10 wt.%, and 20 wt.%) cold-sprayed coatings, respectively. Graphite helps in the formation of tribolayer, and the alumina particles provide load support. The combination of both provides the lowest wear rate for the copper-alumina (10 wt.%)-copper-coated graphite (20 wt.%) cold-sprayed coating. The increase in the amount of graphite in the coatings leads to a lower wear rate of the coating.

In Figure 11, the worn-out cross-section of pure copper, copper-alumina, and copper-alumina (10 wt.%)-copper-coated graphite (10 wt.%) cold-sprayed coatings is presented. As reported and seen in the microstructure, a mixed tribolayer was formed on the pure copper coatings, with a thickness of around 5 – 10 μm with a mixture of large and ultrafine grains, possibly due to the plastic deformation of pure copper. The presence of ultrafine grains improves the plastic deformation and, thereby, the strength and wear resistance of the material. However, the addition of alumina ceramic particles may induce cracks during wear test because of the incompatibility at the ceramic metal matrix interface. However, for the case of copper-alumina (10 wt.%)-copper-

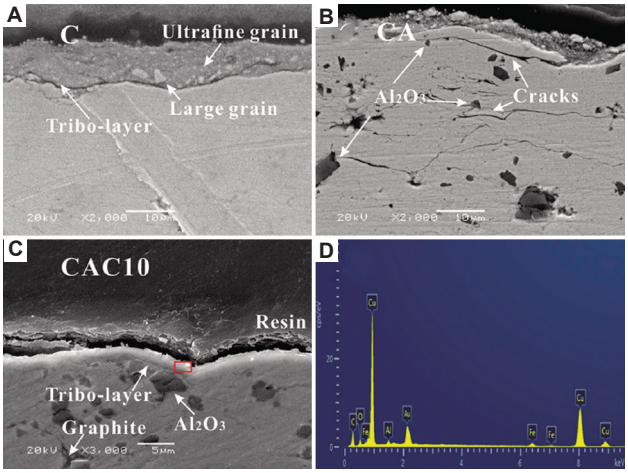

Figure 11. Scanning electron microscopy micrographs of wear cross-section regions in copper-based coatings: (A) Pure copper, (B) copper-alumina (10 wt.%), (C) copper-alumina (10 wt.%)-copper-coated graphite (10 wt.%), and (D) energy-dispersive spectrum of copper-alumina (10 wt.%)-copper-coated graphite (10 wt.%) tribolayer[31]. (Reprinted from *Journal of Thermal Spray Technology*, 27(8), Chen, W., Yu, Y., Cheng, J., Wang, S., Zhu, S., Liu, W., and Yang, J., Microstructure, Mechanical Properties and Dry Sliding Wear Behavior of Cu-Al2O3-Graphite Solid-Lubricating Coatings Deposited by Low-Pressure Cold Spraying, 1652 – 1663, 2018, with permission from Springer Nature).

coated graphite (10 wt.%) cold-sprayed coating, a tribolayer of copper, alumina, and graphite enhanced the solid lubrication, which resulted in no crack formation[31].

4.2. Copper-carbon nanotube (CNTs) coatings

The CNTs have excellent properties such as stiffness, strength, elastic modulus, electrical, and thermal conductivities. Because of the properties of CNTs, the studies on the incorporation of CNTs in composites are widely pursued[6,32-37]. CNTs can be used as reinforcements in improving strength of composites[38-40]. In 2012, Cho *et al.*[41] prepared multi-walled CNT (MWCNT) reinforced copper coatings by cold spray method. As reported, they could substantially avoid the structural damage caused to the CNTs by the low-pressure cold spray process compared to other thermal and high-pressure fabrication processes. In their work, the ball milling process employed to mix the CNTs with copper powder ensured a satisfactory level of mixing of the particles before spraying. The 3 vol.% multi-walled CNT in copper powder feedstock was successfully sprayed onto the aluminum substrate, and the coatings produced had high thermal diffusivity compared to pure copper coatings. The CNTs were homogeneously dispersed in the copper matrix, which accounted for high thermal diffusivity. In some previous reports, the presence of bundled or non-homogeneous dispersion of CNT decreases thermal diffusivity[42,43]. Therefore, Cho *et al.* employed ball milling as an effective strategy to enhance the homogeneous distribution of CNTs in the copper matrix. The MWCNT and copper had good clean and closed interfaces, contributing to low thermal resistance. Furthermore, these were moderately damaged by the ball milling process, which helped retain the desirable properties in the coatings.

In another study, Pialago and Park[44] further increased the amount of CNTs in the copper composite powder feedstock to 15 vol.%. They successfully deposited copper CNT composite powders via cold spray process after ball milling. According to the report, with the increase in the volume percent of CNT reinforcement particles in the feedstock (ranging from 5 to 15 vol.%), the deposition efficiency decreased. Furthermore, the particle size decreases with increasing ceramic content, mostly because the embedded CNTs initiated the cracks during ball milling. This process enhanced the fracturing against the cold welding process of the particles. The cold welding and fracturing of the powder particles may also vary with different milling parameters such as powder composition, size of the balls used, ball-to-powder ratio, and time of milling[44].

Furthermore, from the study by Pialago *et al.*[45], they fabricated copper-based metal matrix composites with CNT and SiC additions (Figure 12). The compositions they made were copper 5%CNT, copper 5%CNT-10%SiC, and copper 5%CNT-20%SiC along with pure copper coatings. As expected, it was reported that with the increase in ceramic content, the fracturing of powder particles (while milling) decreased compared to cold welding, possibly because the CNT and SiC served as crack initiators. Interestingly, the copper 5%CNT-20%SiC was an exception as there was an agglomeration in these powder particles because of increased surface energy due to a reduction in the size of particles. A similar trend was seen in deposition efficiency, where pure copper had the highest deposition efficiency. However, the deposition efficiency decreased with increasing ceramic content for copper 5%CNT and copper 5%CNT-10%SiC. Note that copper 5%CNT-20%SiC had deposition efficiency and coating thickness almost equivalent to pure copper coatings. The reason reported for this exception was the increased amount of ceramics that enhance metal deformation and increase deposition efficiency. Furthermore, copper 5%CNT-20%SiC coatings had the highest hardness, around 240 $Hv_{0.1}$, as compared to all other coatings[45].

The cold spray ternary coatings of copper-CNT-AlN composites were also studied in the literature[46]. These composites were produced by the ball milling mechanical alloying technique. The coating compositions made were copper-5CNT, copper-5CNT-10AlN, copper-10CNT-20AlN, and pure copper (Figure 13). The deposition efficiency reported was highest at around 0.2 for pure

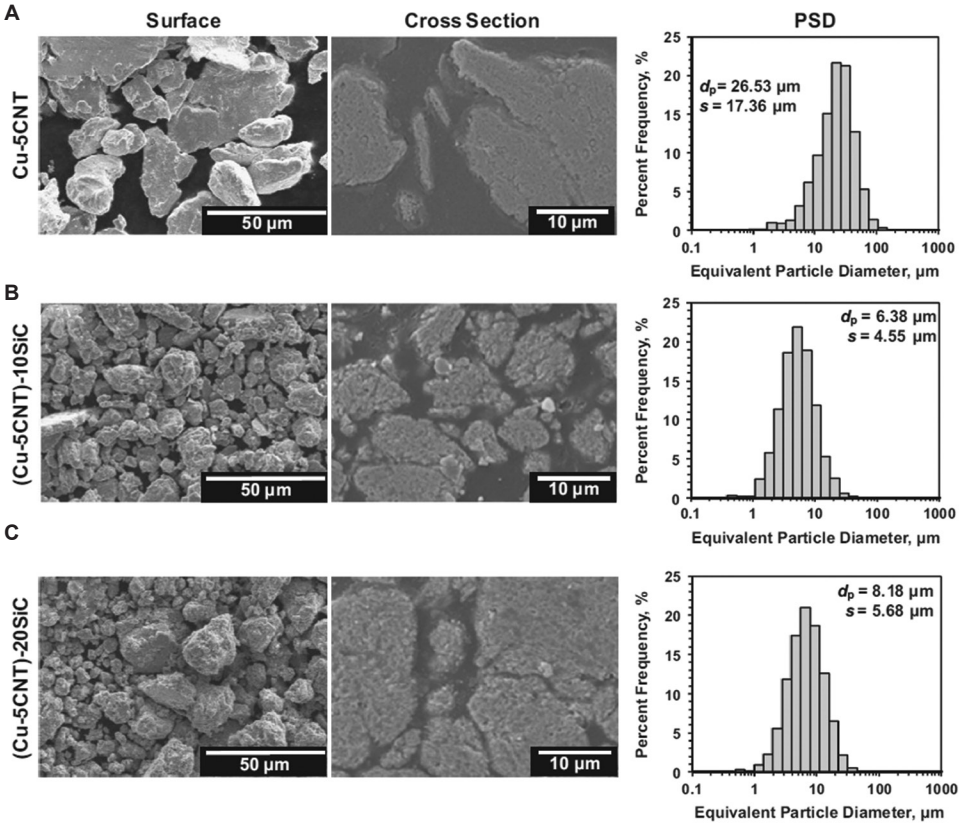

Figure 12. Scanning electron microscopy micrographs and powder size distributions of (A) Cu-5CNT, (B) Cu-5CNT-10SiC, and (C) Cu-5CNT-20SiC[45]. (Reprinted from *Ceramics International*, 41(5), Pialago, E. J. T., Kwon, O. K., and Park, C. W., Cold spray deposition of mechanically alloyed ternary Cu–CNT–SiC composite powders, 6764 – 6775, 2015, with permission from Elsevier).

copper coatings. The deposition efficiency decreased to 0.12 with the addition of CNT (copper 5CNT coatings). However, copper-5CNT-20AlN coatings had slightly better deposition efficiency than copper-5CNT-10AlN coatings. It was also reported that there were small pores in copper-5CNT-10AlN and copper-10CNT-20AlN that open toward the surface as compared to copper-5CNT coatings. Furthermore, copper-5CNT-10AlN coatings were rougher as well as porous than copper-5CNT-20AlN coatings. The pore volumes and surface roughness were the least for copper-5CNT-20AlN coatings compared to the copper-5CNT-10AlN and copper coatings.

4.3. Copper-silicon carbide cermet coatings

Winnicki *et al.*[30] manufactured and studied the corrosion resistance of copper-SiC coatings. In their work, after 18 cycles of salt spray test, the copper SiC coatings showed good corrosion resistance and the buckling of coatings was not so pronounced. As reported by the author, this could be because of the high amount of SiC particles in the coating creating a high amount of ceramic-metal interface, leading to the penetration of chloride ions in them. This effect was not so pronounced in Cu+Al_2O_3 coating work done by Winnicki *et al.* as mentioned above earlier. However, after 18 cycles of Kesternich test in a sulfur dioxide environment, the buckling of copper-SiC coatings was evident. As reported, the electrolyte having the sulfate ions was penetrating into the coating. Furthermore, it was claimed by the author that SiC might be serving as an inert electrode, facilitating the galvanic corrosion, resulting in the delamination of copper-SiC coatings, which is not the case with copper-alumina coatings. This lack of corrosion resistance also resulted in a decrease in the electrical conductivity of as-sprayed copper-SiC coatings. The reported electrical conductivity values were 49% IACS for as-sprayed copper-SiC coatings and around 20% IACS for both cases of corrosion tests (salt spray test and Kesternich test) for copper SiC coatings[30].

Recently, Chen *et al.*[47] cold-sprayed copper-SiC coatings along with pure copper, copper- Al_2O_3, and copper-WC coatings. The compositions made were pure copper, copper-alumina (15 wt.%), copper-SiC (15 wt.%), and copper-WC (15 wt.%). As reported, the density of SiC·Al_2O_3, WC were 3.2 g/cm^3, 3.5 g/cm^3, and 15.63 g/cm^3.

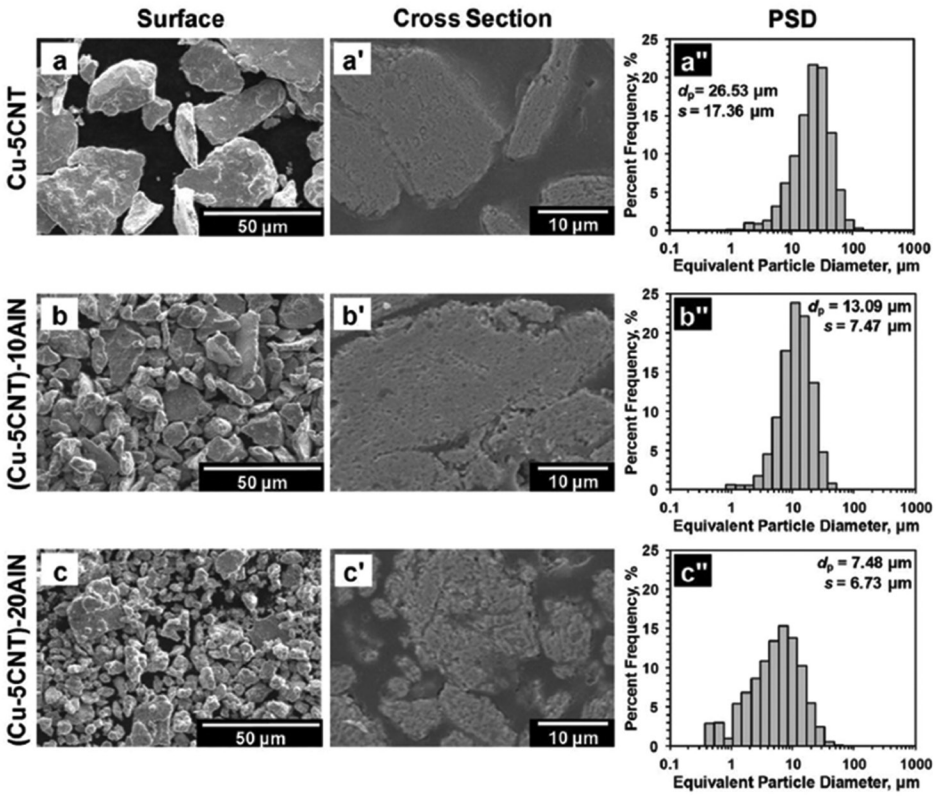

Figure 13. Scanning electron microscopy micrographs and powder size distributions of (A) Cu-5CNT, (B) Cu-5CNT-10AlN, and (C) Cu-5CNT-20AlN[46]. (Reprinted from *Journal of Alloys and Compounds*, 650, Pialago, E. J. T., Kwon, O. K., Kim, M.-S., and Park, C. W., Ternary Cu–CNT–AlN composite coatings consolidated by cold spray deposition of mechanically alloyed powders, 199 – 209, 2015, with permission from Elsevier).

Therefore, due to this density, the deposition of SiC and Al_2O_3 was good enough as compared to the tungsten carbide particles during the cold spray process. The ceramic content of copper-SiC and copper-Al_2O_3 coatings on an average reported was 7.5 + 3.2 vol.% and 10.5 + 2.7 vol.%, respectively. The wear rate of pure copper coatings was 289.57 × 10^{-6} mm^3/Nm and the reported wear rates for copper-SiC and copper-Al_2O_3 cold-sprayed coatings were 207.42 × 10^{-6} mm^3/Nm and 70.88 × 10^{-6} mm^3/Nm, respectively. The microhardness values reported for copper-SiC and copper-Al_2O_3 were 167.36 Hv and 165.01 Hv, which were higher as compared to the cold-sprayed copper coatings around 159.55 Hv. Again, the nanohardness values of copper-SiC and copper-Al_2O_3 coatings are 2.18 GPa and 2.28 GPa, respectively, which are higher than that of pure copper coatings around 2.06 GPa. Furthermore, according to Chen *et al.*, the wear mechanism of pure copper and copper-SiC coatings is adhesive in nature, whereas the copper-Al_2O_3 coatings have an abrasive wear mechanism due to the high bond strength between copper-alumina particles. Furthermore, the thermal conductivities of copper-SiC and copper-Al_2O_3 which were 164.388 W/m-K and 156.911 W/m-K, respectively, at 50°C increased to 209.407 W/m-K and 213.482 W/m-K after the heat treatment of these cold-sprayed coatings. Therefore, the merits of copper-alumina coatings seem to be better, but a thorough research on copper-SiC coatings might bring their characteristic properties into light and prove their commercial importance[47].

4.4. Copper-graphene coatings

Graphene is a wonder material, having excellent electrical conductivity, thermal conductivity, and mechanical strength[48,49]. Good quality graphene can be produced by chemical vapor deposition (CVD) method[50]. Graphene nanoplates (GNPs) are widely used in the production of metal matrix composites as they can be manufactured economically and in large quantities[51]. Yin *et al.*[52] produced GNP-reinforced copper matrix coatings intending to improve anti-friction performance. As reported, ball milling of copper and GNP powders was done; thus, copper-GNP (1 vol.%) powder feedstock was produced. The feedstock was then cold sprayed on an aluminum substrate. Then, a wear test was performed

on pure copper cold spray coatings, cold-sprayed copper GNP (1 vol.%) coatings, and spark plasma sintered copper GNP coatings. Interestingly, the friction coefficient of cold-sprayed copper GNP (1 vol.%) coatings was 20% lesser than that of pure copper cold spray coatings. Furthermore, when compared to spark plasma sintered copper-based coatings, the cold-sprayed copper-GNP coatings performed better at the same volume percent of GNP in the copper matrix. The anti-friction performance was the optimum for copper-GNP cold-sprayed composite coatings. The worn surface of copper-GNP cold-sprayed coatings had very little debris and delamination. The GNPs existing at the worn surface were fractured during the wear test, which provided a graphene-rich film that lubricates the worn surface. Hence, the anti-friction performance is significantly improved[52].

In another work, Choi *et al.*[53] deposited graphene-copper cold spray coatings with copper powders and graphene grown on copper powders by CVD technique. As reported, the copper particles were coated with graphene through CVD process by introducing the powder copper particles to CH_4, H_2, and Ar gases at 100 Pa pressure for 30 min. The graphene-coated copper powder particles were then mixed with pure copper particles at a 1:3 ratio mixture, which was then cold sprayed onto an aluminum plate. The author claims to have created graphene copper composite cold spray coatings with minimal damage to graphene. The possibility of agglomeration due to high surface energy and Van der Waals forces of graphene could also be avoided by the CVD processing technique followed by cold spraying. The damage to graphene that happened during cold spray was evaluated by I_D/I_G ratio through Raman spectroscopy analysis. The I_D/I_G ratio for composite particles was 0.72, which became 0.62 after the cold spray process. This result shows that the damage to graphene was not significant. It is possible that the low temperature of carrier gas could have prevented thermal damage and oxidation of graphene. Furthermore, the band for the graphene also did not shift. It was at the same position 1588 cm^{-1} for both composite powders and coatings, indicating very low compressive residual stress induced during the cold spray process. The interatomic forces between graphene and copper particles due to the high electron density at the interface between copper and graphene prevented the pullout of graphene

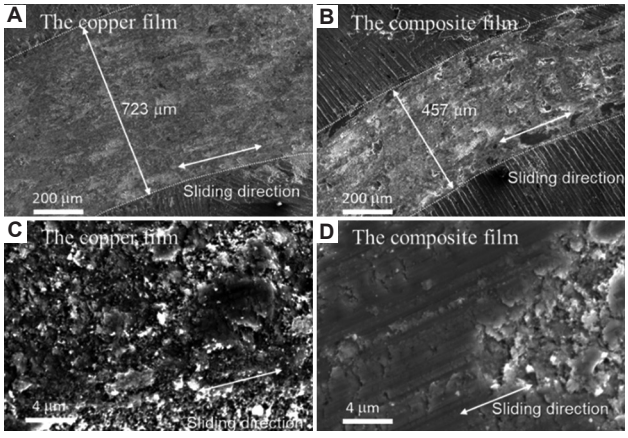

Figure 14. Scanning electron microscopy micrographs of sliding mark on the copper surface and composite film surface[53]. (Reprinted from *Diamond and Related Materials*, 116, Choi, J., Okimura, N., Yamada, T., Hirata, Y., Ohtake, N., and Akasaka, H., Deposition of graphene-copper composite film by cold spray from particles with graphene grown on copper particles, 108384, 2021, with permission from Elsevier).

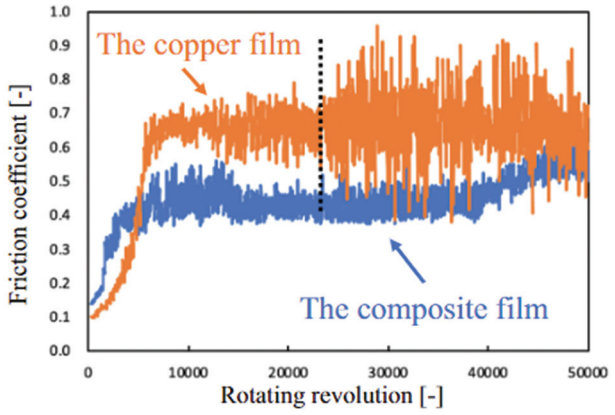

Figure 15. The measured coefficient of friction for copper and composite film[53]. (Reprinted from Diamond and Related Materials, 116, Choi, J., Okimura, N., Yamada, T., Hirata, Y., Ohtake, N., and Akasaka, H., Deposition of graphene-copper composite film by cold spray from particles with graphene grown on copper particles, 108384, 2021, with permission from Elsevier).

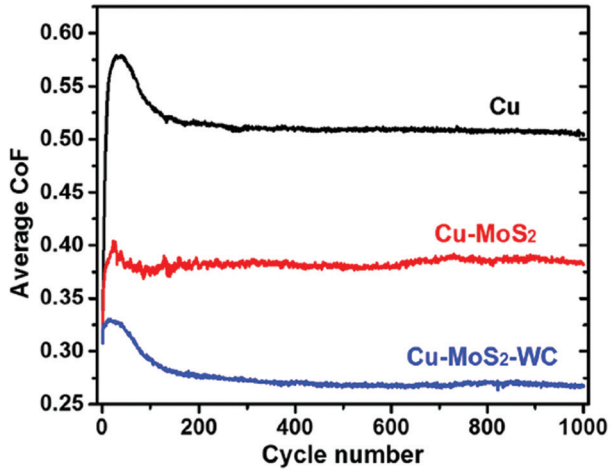

Figure 16. Coefficient of friction for copper, copper-MoS_2, and copper-MoS_2-WC[63]. (Reprinted from *Tribology International*, 123, Zhang, Y., Epshteyn, Y., and Chromik, R. R., Dry sliding wear behavior of cold-sprayed Cu-MoS2 and Cu-MoS2-WC composite coatings: The influence of WC, 296 – 306, 2018, with permission from Elsevier).

from copper particles by the Van der Waals forces, which became an advantage for cold spraying and enhanced wear resistance characteristics[53].

In Figure 14, worn areas of copper and its composite coatings are shown[53]. The graphene copper composite coatings had a better friction coefficient of 0.46, and copper coatings had a friction coefficient of 0.6, as shown in Figure 15. Furthermore, the wear rates for graphene copper composite coatings were 5.2×10^{-4} mm^3/Nm and that for pure copper coatings were 8.6×10^{-4} mm^3/Nm[53].

4.5. Copper-MoS_2 composite coatings

Metal matrix composites that have good wear resistance and self-lubricating properties can be used for making bearings[54]. In this material type, MoS_2 particles can play an effective role in reducing friction and wear rate[55]. The addition of ceramic particles into self-lubricating metal matrix composites is a good practice to ameliorate the wear resistance and strength of these composites[56-61]. Moreover, cold spray can be a beneficial method for spraying metal matrix composites powder feedstock containing MoS_2 because there could be no decomposition or phase transformations of solid lubricant MoS_2 as the cold spray process does not involve very high temperatures. Brittle compounds such as Cu_2S and $CuMo_2S_3$ may cause an increase in friction and wear, eliminating the purpose of solid lubricant when the Cu-MoS_2 composites are fabricated through sintering[62].

Zhang *et al.*[63] studied the sliding wear behavior of copper-MoS_2 and copper-MoS_2-WC cold spray coatings. As reported, the sliding wear experiment done showed that copper-MoS_2-WC coatings had low friction and wear rate compared to copper-MoS_2 coatings. The tungsten carbide particles helped reduce the friction; wear became uniform throughout the wear track, as shown in Figure 16. The tungsten carbide particles embedded in the coating had a thin layer of copper, which could be an advantage because the function of hard particles like tungsten carbide is not only to reduce friction but also to not serve as abrasives during wearing by having direct contact. In that work, the authors did not use a high volume percent of tungsten carbide in the coatings; probably, because tungsten carbide particles can compromise the bond strength. As far as copper-MoS_2 coatings were concerned, the MoS_2 particles smeared out during sliding and replenishing the particles continued with sliding. However, for copper-MoS_2-WC coatings, more wear debris accumulation due to WC particles suggests a low wear rate. There was an active transfer of material due to rapid wear debris removal in the case of copper-MoS_2 coatings. This led to detachments and cracks on copper-MoS_2 wear tracks, which was not observed in copper-MoS_2-WC wear track. Furthermore, the subsurface microstructures of copper-MoS_2-WC wear tracks suggested that the WC particles also served as load bearers and protected the rest of the surface from severe plastic deformation. The presence of the ultrafine grains only around the WC particles proved it. While for the copper-MoS_2 coatings, the ultrafine grains were present everywhere on the worn surface. The cracks on copper-MoS_2 wear tracks were again due to the already work hardened ultrafine grains present all over the surface of the wear track.

4.6. Copper-TiB_2 composite coatings

Copper-TiB_2 composite fabrication has received much attention due to its vivid applications that require properties such as electrical conductivity, thermal conductivity, wear

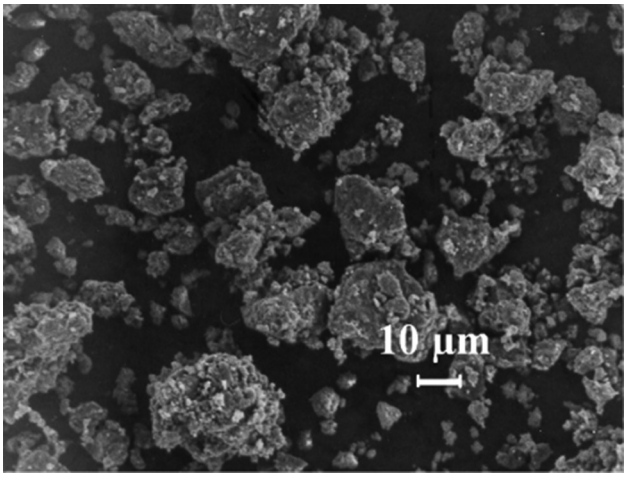

Figure 17. Copper-43 vol.% TiB_2 feedstock powders formed as product after the SHS reaction for cold spraying[70]. (Reprinted from *Composites Science and Technology*, 67(11), Kim, J. S., Kwon, Y. S., Lomovsky, O. I., Dudina, D. V., Kosarev, V. F., Klinkov, S. V., Kwon, D. H., and Smurov, I., Cold spraying of *in situ* produced TiB2–Cu nanocomposite powders, 2292 – 2296, 2007, with permission from Elsevier).

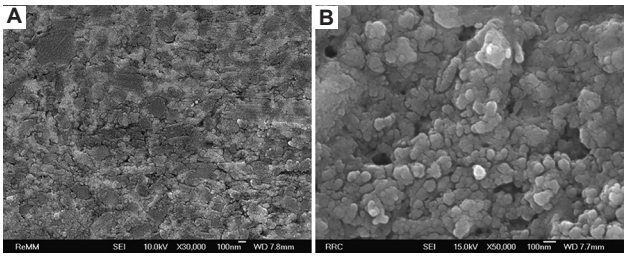

Figure 18. Microstructures of copper-43 vol.% TiB_2 cold spray coating: (A) Etched with $(NH_4)_2S_2O_8$ aqueous solution and (B) etched with $FeCl_3$ aqueous solution[70]. (Reprinted from *Composites Science and Technology*, 67(11), Kim, J. S., Kwon, Y. S., Lomovsky, O. I., Dudina, D. V., Kosarev, V. F., Klinkov, S. V., Kwon, D. H., and Smurov, I., Cold spraying of *in situ* produced TiB2–Cu nanocomposite powders, 2292 – 2296, 2007, with permission from Elsevier).

resistance, and strength[64-68]. Titanium diboride particles do not react with copper; it has a high melting point, high strength, resistance to wear, and hardness[69], which make them attractive for applications in the electrical industry[66,70].

In 2007, Kim *et al.*[70] were successful in spraying copper-43 vol.% TiB_2. As reported, titanium, boron, and copper nanocomposite powders were subjected to ball milling for 2 min and then subjected to self-propagating high-temperature synthesis reaction (SHS). Further, the product obtained after self-propagating high-temperature synthesis reaction was milled again to obtain optimum size TiB_2 particles, as shown in Figure 17. The heat of the SHS reaction got distributed evenly all around due to the good thermal conductivity of copper, which helped in the proper formation of TiB_2 particles. This powder feedstock was sprayed onto a copper substrate. The cold-sprayed coating was reported to be 70 µm in thickness. The coatings were very dense, possibly due to the huge plasticity difference between the copper and TiB_2 in these coatings. As reported, the coatings etched with $(NH_4)_2S_2O_8$ aqueous solution, as shown in Figure 18A, display the microstructure of the composite coating. The powder particles are closely packed in the coatings. Furthermore, in Figure 18B, the coatings etched with $FeCl_3$ solution are shown where the selective removal of copper from the surface leaves behind the network of TiB_2 phase. The Vickers hardness of copper-43 vol.% TiB_2 coating was reported to be 378 Hv which was much higher than that of the pure copper cold spray coatings, having a Vickers hardness of around 159.55 Hv as reported by Chen *et al.*[47]. The titanium diboride structure is responsible for the high hardness of copper-43 vol.% TiB_2 cold-sprayed coatings.

In another work, Calli *et al.*[71] produced cold-sprayed pure copper, copper-B_4C, copper-TiB_2, and copper-TiC coatings. As reported, the electrical conductivity of pure copper coatings was equivalent to that of the copper-TiB_2 (12.5 vol.%), around 36.0 MS/m, which is more than that of the copper-B_4C (12.5 vol.%) coatings and copper TiC (12.5 vol.%). This observation may be due to the electrical conductivity of the ceramic particles used. However, the relative wear rates (RWRs) were lowest for copper-TiB_2 coatings compared to copper-TiC and copper-B_4C coatings. This result could be due to the third

Table 1. Summary of cold spray deposition parameters for copper-based cold spray coatings

Powder	Composition	Particle diameter (µm)	Gas	Po	To	SoD (mm)	Q (g/min)	Substrate	Ref.
Copper	Pure copper	Cu (ACU 325)	N_2	2.8 MPa	500°C	35	32.1+1.14	Cu	[45]
Cu-Al_2O_3	Cu 90,70,50 Al2O3 10, 30, 50	25+5	Air	6 bar	540°C	10	-	Steel	[30]
Cu-Al_2O_3 – Cu coated graphite	Cu (90, 85, 80, and 70 wt.%), Al_2O_3 (10 wt.%), Cu coated graphite (0, 5, 10, and 20 wt.%)	Cu (20.18 µm), Al_2O_3 (4.41 µm), Cu coated graphite (47.77 µm)	Air	0.8 MPa	500°C	10	14 – 16	304SS	[31]
Cu-CNT	Cu 100, 95, 90, 85 CNT 0, 5, 10, 15	10 – 30	N_2	2.8 MPa	500°C	35	22.51 – 28.88	-	[44]
Cu-CNT-SiC	Cu (95 vol.%)-CNT (5 vol.%) SiC (10 and 20 vol.%)	Cu (ACU 325) CNT (5 – 20 nm) SiC (320 grit)	N_2	2.8 MPa	500°C	35	23.60 – 28.88	Cu	[45]
Cu-CNT-AlN	Cu (95 vol.%)-CNT (5 vol.%) AlN (10 and 20 vol.%)	Cu (ACU 325) CNT (5 – 20 nm) AlN (7 – 30 µm)	N_2	2.8 MPa	500°C	35	21.95 – 28.88	Cu	[46]
Cu- MwCNT	Cu (97 vol.%) MwCNT (3 vol.%)	0.5 – 3	Air	0.6 MPa	200°C	-	-	Al	[41]
Cu-graphene	Cu (99 vol.%) Graphene (1 vol.%)	Cu 15-38 µm Graphene 5 – 30 nm	He	2 MPa	25°C	40	-	Al	[52]
Cu-graphene	Pure copper powder coated with graphene	20	Air	0.6 MPa	720 K	12	8.21	Al	[53]
Cu-MoS_2	Cu 85 vol.%/MoS_2 (15 vol.%)	Cu (26 µm) MoS_2 (68 µm)	N_2	5 MPa	800°C	-	Cu (34.8) MoS_2 (3.6)	AA6061	[63]
Cu-MoS_2-WC	Cu 85 vol.%, MoS_2 (14 vol.%), WC (11 vol.%)	Cu (26 µm) MoS_2 (68 µm) WC (30 µm)	N_2	5 MPa	800°C	-	Cu+WC (39.4) MoS_2 (3.6)	AA6061	[63]

body abrasion mechanism, which happens due to the detachment of ceramic particles that break the oxide layer of metal during wear tests. The reported RWRs were 1.0, 2.7, 3.13, and 5.95 for pure copper, copper-TiB_2, copper B_4C, and copper TiC coatings, respectively. The coating thickness obtained for copper TiB_2 coatings was 1690 μm, which was much higher than that of pure copper (825 μm), copper B_4C (270 μm), and copper TiC (550 μm).

5. Cold spray deposition parameters and properties of copper-based cold spray coatings

Different reinforcements such as Al_2O_3, graphite, CNT, WC, MoS_2, and TiB_2 provide different properties to the copper-based cold spray coatings. These properties vary with the number of reinforcements employed, the morphology of powder particles, deposition conditions implemented, interface bonding characteristics, and characteristic properties of reinforcements. Table 1 shows the deposition parameters and compositions of the copper-based cold spray coatings and their substrates in the literature. The particle diameter generally preferred for copper-based cold spray coatings is between 10 μm and 50 μm to ensure good deposition efficiency. The low deposition temperatures also ensure that changes in the structural and mechanical properties are also minimized, and the purpose of the addition of ceramic particles is accomplished. The gases used for cold spray deposition have been helium, nitrogen, and air. Helium and nitrogen generally can help reduce oxidation. However, the authors who utilized air for cold spray deposition did not report any considerable oxidation of powder particles. The various substrates used for cold spray deposition in the references by different authors depend on various possible industrial applications of these coatings according to commercial acceptance. The applications of such copper-based cold spray coatings can be for seam and spot welding electrodes, conductors used for high-temperature applications, lead wires, electrical contacts, switches, etc.[29] Every material used as a reinforcement in the copper-based cold spray coatings serves its intended purpose.

In Table 2, a summary of the properties of various copper-based cold spray coatings with different reinforcements in the literature is presented. Numerous tests have been conducted by different authors to verify the effect of

Table 2. Comparison of various properties of copper-based cold spray coatings

Powder	Composition	Electrical conductivity	Friction coefficient	Wear rates	Microhardness	Ref.
Copper	Pure copper	36 MS/m	0.6	8.6×10^{-4}	140 – 160 Hv0.3	[23,53,71]
Cu-Al_2O_3	Cu (50 wt.%), Al_2O_3 (50 wt.%)	62% IACS	-	-	83 – 127 Hv0.3	[30]
Cu-Al_2O_3 – Cu coated graphite	Cu (90, 85, 80, and 70 wt.%), Al_2O_3 (10 wt.%) Cu-coated graphite (0, 5, 10, and 20 wt.%)	-	0.34 – 0.94	2.53×10^{-4} to 1.2×10^{-4}	114.3 – 88.2 Brinell hardness	[31]
Cu-CNT	Cu 100, 95, 90, 85 CNT 0, 5, 10, 15	-	-	-	160 – 230 Hv0.1	[45]
Cu-CNT-SiC	Cu (95 vol.%)-CNT (5 vol.%) SiC (10 and 20 vol.%)	-	-	-	190 – 260 Hv0.1	[45]
Cu- MwCNT	Cu (97 vol.%) MwCNT (3 vol.%)	-	-	-	303.64	[41]
Cu-graphene	Pure copper powder coated with graphene		0.46	5.2×10^{-4}		[53]
Cu-MoS_2	Cu 85 vol.%/MoS_2 (15 vol.%)	-	0.38 – 0.4	210×10^{-6} to 35×10^{-6}	75 – 132 Hv0.2	[63]
Cu-MoS_2-WC	Cu 85 vol.%, MoS_2 (14 vol.%), WC (11 vol.%)	-	0.27 – 0.33	123×10^{-6} to 19×10^{-6}	87 – 135 Hv0.2	[63]
Cu-TiB_2	Cu-12.5 vol% TiB_2	36 MS/m	-	Relative wear rate (with pure copper as 1) 2.7	156 Hv 0.025	[71]
Cu-B_4C	Cu-12.5 vol% TiB_2	34.3 MS/m	-	Relative wear rate (with pure copper as 1) 3.13	151 Hv 0.025	[71]
Cu-TiB_2	Cu-12.5 vol% TiB_2	35.6 MS/m	-	Relative wear rate (with pure copper as 1) 5.95	157 Hv 0.025	[71]

reinforcements in copper-based cold spray coatings. The electrical conductivity of pure copper and copper-based cold spray coatings considerably depends on the deposition parameters and porosity in the coatings. In general, higher porosity leads to lower electrical conductivity. The addition of reinforcements may or may not contribute to the increase in electrical conductivity, possibly due to the ineffectiveness of deposition, effective deformation of copper matrix, the amount of reinforcement used, and characteristic property of the reinforcements. Another property with commercial importance is the friction coefficient and wear rate. The addition of reinforcements such as graphite and MoS_2 imparts good lubrication properties, which decreases the friction coefficient and wear rates of the copper-based cold spray coatings. However, in such coatings, there could be a decrease in hardness values, possibly due to the weak interface bonding between metal matrix and reinforcement. Furthermore, this decrease in microhardness trend was not visible for reinforcements specifically used to improve the strength and hardness of copper-based cold spray coatings.

6. Conclusions and scope for future work

Pure copper and copper-based cold spray coatings are an interesting area of research in power industries. Copper-based cold spray coatings can enhance electrical and thermal conductivity, wear, and corrosion resistance, along with proper hardness and strength of components. The deposition parameters required for the cold spray of the copper-based coatings discussed in this work mainly consist of the gases used for cold spray, the pressure of the gas, standoff distance, and powder feedstock preparation for cold spraying by milling process with the incorporation of surfactants. Surfactants play a huge role in powder preparation, according to the size range required for cold spraying process. The mechanical milling process is an effective method to produce powder feedstock with homogeneity. The homogeneous distribution of reinforcement particles in the metallic copper matrix provides uniform mechanical and tribological properties.

Numerous research works focused on different types of reinforcements in copper-based cold spray coatings have been done. These different reinforcements provide unique properties to the copper-based coating according to their characteristics. The deformation and recrystallization of copper grains in pure copper coatings have been focused on in this work, along with the variation in properties with different amounts of reinforcements have also been discussed. These reinforcements have also been responsible for increasing the deposition efficiency and significant reduction in porosity. The copper-based cold spray coatings have shown superior qualities in terms of wear resistance, lesser oxidation, hardness, electrical conductivity, and so on when compared to other coating processes. The cold-sprayed copper coatings also retained the inherent characteristic properties of reinforcements without causing much damage to the reinforcements. This could be because of the low operating temperatures of the cold spray process that avoids any kind of melting or oxidation.

Copper-based cold spray coatings have immense scope for the future research works. The correct type and amount of reinforcements that can give the best desirable properties for copper-based coatings must be explored. The deposition efficiency of these copper-based coatings with the help of powder architecture and powder morphology is yet to be investigated thoroughly. The higher the deposition efficiency, the lesser wastage of powder feedstock used for the cold spraying process. Recycling of process gases and feedstock powder from economic and environmental point of view is important, and research on it is inevitable. The research works must include the incorporation of two reinforcements in the metal matrix that can provide enhanced mechanical and tribological properties. The electrical and thermal properties of copper-based cermets according to the various reinforcements used are a matter of further investigation, and this can be compared with the other coating processes such as HVOF, CVD, sintering, and so on. The comparisons can also be made among the various copper-based cold-sprayed coatings with several types of reinforcements. A thorough investigation of preserving the original grain sizes desired phases, and the chemistry of materials is desirable. The research works on bond strength and bonding characteristics, fatigue strength, thermal shock resistance, oxidation, and corrosion resistance of copper-based cold spray coatings can be beneficial in creating worthwhile coatings having great commercial importance.

Acknowledgments

The authors acknowledge with gratitude funding received from the Natural Sciences and Engineering Research Council of Canada (NSERC), the Canada Foundation for Innovation (CFI), Transport Canada, and the New Brunswick Innovation Foundation (NBIF).

Funding

This work is funded by the NSERC, the CFI, Transport Canada, and the NBIF.

Conflict of interest

The authors have no conflicts of interest to declare that are relevant to the content of this article.

Author contributions

Conceptualization: Vineeth Menon, Clodualdo Aranas Jr., and Gobinda Saha
Data curation: Vineeth Menon
Funding acquisition: Clodualdo Aranas Jr. and Gobinda Saha
Supervision: Clodualdo Aranas Jr. and Gobinda Saha
Writing – original draft: Vineeth Menon
Writing – review and editing: Clodualdo Aranas Jr. and Gobinda Saha.

References

1. Alkhimov AP, Papyrin AN, Kosarev VF, *et al.*, 1994, Gas-dynamic spraying method for applying a coating (United States Patent No. US5302414A). Available from: https://patents.google.com/patent/US5302414A/en [Last accessed on 2022 May 31].
2. Tokarev AO, 1996, Structure of aluminum powder coatings prepared by cold gasdynamic spraying. *Metal Sci Heat Treat*, 38: 136–139. https://doi.org/10.1007/BF01401446
3. Sripada J, Gallant M, Saha G, 2019, Study on the effect of milling parameters on HE-MA nanostructured Al-graphene cermet particles. *Proceedings of 1st Coatings and Interfaces Web Conference, 2019*, 6160. https://doi.org/10.3390/ciwc2019-06160
4. McCune RC, Donlon WT, Popoola OO, *et al.*, 2000, Characterization of copper layers produced by cold gas-dynamic spraying. *J Therm Spray Technol*, 9: 73–82. https://doi.org/10.1361/105996300770350087
5. Woo DJ, Heer FC, Brewer LN, *et al.*, 2015, Synthesis of nanodiamond-reinforced aluminum metal matrix composites using cold-spray deposition. *Carbon*, 86: 15–25. https://doi.org/10.1016/j.carbon.2015.01.010
6. Popovich A, Sufiiarov V, 2016. Metal powder additive manufacturing. In: Shishkovsky IV, editor. New Trends in 3D Printing. InTech, London. https://doi.org/10.5772/63337
7. Raoelison RN, Xie Y, Sapanathan T, *et al.*, 2018, Cold gas dynamic spray technology: A comprehensive review of processing conditions for various technological developments till to date. *Addit Manuf*, 19: 134–159. https://doi.org/10.1016/j.addma.2017.07.001
8. Stoltenhoff T, Kreye H, Richter HJ, 2002, An analysis of the cold spray process and its coatings. *J Therm Spray Technol*, 11: 542–550. https://doi.org/10.1361/105996302770348682
9. Suryanarayana C, 2001, Mechanical alloying and milling. *Prog Mater Sci*, 46: 1–184. https://doi.org/10.1016/S0079-6425(99)00010-9
10. Zhang DL, 2004, Processing of advanced materials using high-energy mechanical milling. *Prog Mater Sci*, 3–4: 537–560. https://doi.org/10.1016/S0079-6425(03)00034-3
11. Sripada JV, Saha DC, Saha GC, *et al.*, 2021, Study the effect of milling parameters on HE-MA nanostructured Al6061-graphene cermet feedstock particles. *J Alloys Comp*, 859: 157759. https://doi.org/10.1016/j.jallcom.2020.157759
12. Hu Z, Chen F, Xu J, *et al.*, 2018, 3D printing graphene-aluminum nanocomposites. *J Alloys Comp*, 746: 269–276. https://doi.org/10.1016/j.jallcom.2018.02.272
13. Toozandehjani M, Matori KA, Ostovan F, *et al.*, 2017, Effect of milling time on the microstructure, physical and mechanical properties of Al-Al_2O_3 nanocomposite synthesized by ball milling and powder metallurgy. *Materials*, 10: 1232. https://doi.org/10.3390/ma10111232
14. Nouri A, Wen C, 2014, Surfactants in mechanical alloying/milling: A catch-22 situation. *Crit Rev Solid State Mater Sci*, 39: 81–108. https://doi.org/10.1080/10408436.2013.808985
15. Kollo L, Leparoux M, Bradbury CR, *et al.*, 2010, Investigation of planetary milling for nano-silicon carbide reinforced aluminium metal matrix composites. *J Alloys Comp*, 489: 394–400. https://doi.org/10.1016/j.jallcom.2009.09.128
16. Lu L, Zhang YF, 1999, Influence of process control agent on interdiffusion between Al and Mg during mechanical alloying. *J Alloys Comp*, 290: 279–283. https://doi.org/10.1016/S0925-8388(99)00221-2
17. Shaw L, Villegas J, Luo H, *et al.*, 2003, Effects of process-control agents on mechanical alloying of nanostructured aluminum alloys. *Metallurgical Mater Trans A Phys Metallurgy Mater Sci*, 34: 159–170. https://doi.org/10.1007/s11661-003-0217-7
18. Legoux JG, Irissou E, Desaulniers S, *et al.*, n.d., Characterization and Performance Evaluation of a Helium Recovery System Designed for Cold Spraying. National Research Council Canada, Canada.
19. Cao K, Yu M, Liang CM, *et al.*, 2020, Study on thermal conductivity of cold sprayed Cu coating. *Surface Eng*, 36: 1058–1066. https://doi.org/10.1080/02670844.2020.1790170
20. Yin S, Xie Y, Cizek J, *et al.*, 2017, Advanced diamond-reinforced metal matrix composites via cold spray: Properties and deposition mechanism. *Compos B Eng*, 113: 44–54. https://doi.org/10.1016/j.compositesb.2017.01.009

21. Imbriglio SI, Chromik RR., 2021, Factors affecting adhesion in metal/ceramic interfaces created by cold spray. *J Therm Spray Technol*, 30: 1703–1723.

    https://doi.org/10.1007/s11666-021-01229-4

22. Pathak S, Saha GC., 2017, Development of sustainable cold spray coatings and 3D additive manufacturing components for repair/manufacturing applications: A critical review. *Coatings*, 7: 122.

    https://doi.org/10.3390/coatings7080122

23. Fukumoto M, Wada H, Tanabe K, *et al*., 2007, Effect of substrate temperature on deposition behavior of copper particles on substrate surfaces in the cold spray process. *J Therm Spray Technol*, 16: 643–650.

    https://doi.org/10.1007/s11666-007-9121-9

24. Borchers C, Stoltenhoff T, Gärtner F, *et al*., 2001, Deformation microstructure of cold gas sprayed coatings. *Mater Res Soc Symp Proc*, 674: P7.10.1–P.10.6.

    https://doi.org/10.1557/proc-673-p7.10

25. Assadi H, Kreye H, Gärtner F, *et al*., 2016, Cold spraying a materials perspective. *Acta Materi*, 116: 382–407.

    https://doi.org/10.1016/j.actamat.2016.06.034

26. Moridi A, Hassani-Gangaraj SM, Guagliano M, *et al*., 2014, Cold spray coating: Review of material systems and future perspectives. *Surface Eng*, 30: 369–395.

    https://doi.org/10.1179/1743294414Y.0000000270

27. Winnicki M, Małachowska A, Piwowarczyk T, *et al*., 2016, The bond strength of Al + Al_2O_3 cermet coatings deposited by low-pressure cold spraying. *Arch Civil Mech Eng*, 16: 743–752.

    https://doi.org/10.1016/j.acme.2016.04.014

28. Koivuluoto H, Vuoristo P, 2010, Effect of powder type and composition on structure and mechanical properties of Cu + Al_2O_3 coatings prepared by using low-pressure cold spray process. *J Therm Spray Technol*, 19: 1081–1092.

    https://doi.org/10.1007/s11666-010-9491-2

29. Phani PS, Vishnukanthan V, Sundararajan G, 2007, Effect of heat treatment on properties of cold sprayed nanocrystalline copper alumina coatings. *Acta Mater*, 55: 4741–4751.

    https://doi.org/10.1016/j.actamat.2007.04.044

30. Winnicki M, Baszczuk A, Jasiorski M, *et al*., 2017, Corrosion resistance of copper coatings deposited by cold spraying. *J Therm Spray Technol*, 26: 1935–1946.

    https://doi.org/10.1007/s11666-017-0646-2

31. Chen W, Yu Y, Cheng J, *et al*., 2018, Microstructure, mechanical properties and dry sliding wear behavior of Cu-Al_2O_3-graphite solid-lubricating coatings deposited by low-pressure cold spraying. *J Therm Spray Technol*, 27: 1652–1663.

    https://doi.org/10.1007/s11666-018-0773-4

32. Zhan GD, Kuntz JD, Wan J, *et al*., 2003, Single-wall carbon nanotubes as attractive toughening agents in alumina-based nanocomposites. *Nat Mater*, 2: 38–42.

    https://doi.org/10.1038/nmat793

33. Coleman JN, Khan U, Blau WJ, *et al*., 2006, Small but strong: A review of the mechanical properties of carbon nanotube-polymer composites. *Carbon*, 44: 1624–1652.

    https://doi.org/10.1016/j.carbon.2006.02.038

34. Ajayan PM, Tour JM, 2007, Nanotube composites. *Nature*, 447: 1066–1068.

    https://doi.org/10.1038/4471066a

35. Kwon H, Estili M, Takagi K, *et al*., 2009, Combination of hot extrusion and spark plasma sintering for producing carbon nanotube reinforced aluminum matrix composites. *Carbon*, 47: 570–577.

    https://doi.org/10.1016/j.carbon.2008.10.041

36. Cha SI, Kim KT, Arshad SN, *et al*., 2005, Extraordinary strengthening effect of carbon nanotubes in metal-matrix nanocomposites processed by molecular-level mixing. *Adv Mater*, 17: 1377–1381.

    https://doi.org/10.1002/adma.200401933

37. Bakshi SR, Lahiri D, Agarwal A, 2010, Carbon nanotube reinforced metal matrix composites a review. *Int Mater Rev*, 55: 41–64.

    https://doi.org/10.1179/095066009X12572530170543

38. Shukla AK, Nayan N, Murty SV, *et al*., 2013, Processing of copper-carbon nanotube composites by vacuum hot pressing technique. *Mater Sci Eng A*, 560: 365–371.

    https://doi.org/10.1016/j.msea.2012.09.080

39. Kang K, Bae G, Won J, *et al*., 2012, Mechanical property enhancement of kinetic sprayed Al coatings reinforced by multi-walled carbon nanotubes. *Acta Mater*, 60: 5031–5039.

    https://doi.org/10.1016/j.actamat.2012.05.034

40. Xie X, Chen C, Ji G, *et al*., 2019, A novel approach for fabricating a CNT/AlSi composite with the self-aligned nacre-like architecture by cold spraying. *Nano Mater Sci*, 1: 137–141.

    https://doi.org/10.1016/j.nanoms.2019.04.002

41. Cho S, Takagi K, Kwon H, *et al*., 2012, Multi-walled carbon nanotube-reinforced copper nanocomposite coating fabricated by low-pressure cold spray process. *Surf Coat Technol*, 206: 3488–3494.

    https://doi.org/10.1016/j.surfcoat.2012.02.021

42. Kim P, Shi L, Majumdar A, *et al*., 2001, Thermal transport measurements of individual multiwalled nanotubes. *Phys Rev Lett*, 87: 215502.

    https://doi.org/10.1103/PhysRevLett.87.215502

43. Cho S, Kikuchi K, Miyazaki T, *et al*., 2010, Multiwalled carbon nanotubes as a contributing reinforcement phase for the improvement of thermal conductivity in copper matrix composites. *Sci Mater*, 63: 375–378.

    https://doi.org/10.1016/j.scriptamat.2010.04.024

44. Pialago EJ, Park C. Cold spray deposition characteristics of mechanically alloyed Cu-CNT composite powders. *Appl Surf Sci*, 308: 63–74.

    https://doi.org/10.1016/J.APSUSC.2014.04.096

45. Pialago EJ, Kwon OK, Park CW, 2015, Cold spray deposition of mechanically alloyed ternary Cu-CNT-SiC composite powders. *Ceram Int*, 41: 6764–6775.

    https://doi.org/10.1016/j.ceramint.2015.01.123

46. Pialago EJ, Kwon OK, Kim MS, *et al*., 2015, Ternary Cu-CNT-AlN composite coatings consolidated by cold spray deposition of mechanically alloyed powders. *J Alloys Comp*, 650: 199–209.

    https://doi.org/10.1016/j.jallcom.2015.08.007

47. Chen Q, Yu M, Cao K, *et al*., 2022, Thermal conductivity and wear resistance of cold sprayed Cu-ceramic phase composite coating. *Surf Coat Technol*, 434: 128135.

    https://doi.org/10.1016/j.surfcoat.2022.128135

48. Novoselov KS, Geim AK, Morozov SV, *et al*., 2004, Electric field effect in atomically thin carbon films. *Science*, 306: 666–669.

    https://doi.org/10.1126/science.1102896

49. Warner JH, Schaffel F, Rummeli M, *et al*., 2012, Graphene: Fundamentals and Emergent Applications. Elsevier, Amsterdam, Netherlands, p61-125.

50. Reina A, Jia X, Ho J, *et al*., 2009, Large area, few-layer graphene films on arbitrary substrates by chemical vapor deposition. *Nano Lett*, 9: 30–35.

    https://doi.org/10.1021/nl801827v

51. Kotov NA, 2006, Carbon sheet solutions. *Nature*, 442: 254–255.

    https://doi.org/10.1038/442254a

52. Yin S, Zhang Z, Ekoi EJ, *et al*., 2017, Novel cold spray for fabricating graphene-reinforced metal matrix composites. *Mater Lett*, 196: 172–175.

    https://doi.org/10.1016/j.matlet.2017.03.018

53. Choi J, Okimura N, Yamada T, *et al*., 2021, Deposition of graphene-copper composite film by cold spray from particles with graphene grown on copper particles. *Diam Relat Mater*, 116: 108384.

    https://doi.org/10.1016/j.diamond.2021.108384

54. Chromik R, Alidokht S, Shockley JM, *et al*., 2018, Tribological coatings prepared by cold spray. In: Cold-Spray Coatings. Springer, Berlin, p321–348.

    https://doi.org/10.1007/978-3-319-67183-3_11

55. Wu Y, Wang F, Cheng Y, *et al*., 1997, A study of the optimization mechanism of solid lubricant concentration in $NiMoS_2$ self-lubricating composite. *Wear*, 205: 64–70.

    https://doi.org/10.1016/S0043-1648(96)07299-7

56. Miracle DB, 2005, Metal matrix composites from science to technological significance. *Comp Sci Technol*, 65: 2526–2540.

    https://doi.org/10.1016/j.compscitech.2005.05.027

57. Suresha S, Sridhara BK, 2010b, Wear characteristics of hybrid aluminium matrix composites reinforced with graphite and silicon carbide particulates. *Comp Sci Technol*, 70: 1652–1659.

    https://doi.org/10.1016/j.compscitech.2010.06.013

58. Narayanasamy P, Selvakumar N, Balasundar P, 2015, Effect of hybridizing MoS_2 on the tribological behaviour of Mg-TiC composites. *Trans Indian Inst Metals*, 68:911–925.

    https://doi.org/10.1007/s12666-015-0530-z

59. Xu J, Liu W, Zhong M, 2006, Microstructure and dry sliding wear behavior of MoS_2/TiC/Ni composite coatings prepared by laser cladding. *Surf Coat Technol*, 200: 4227–4232.

    https://doi.org/10.1016/j.surfcoat.2005.01.036

60. Rajkumar K, Aravindan S, 2011, Tribological performance of microwave sintered copper-TiC-graphite hybrid composites. *Tribol Int*, 44: 347–358.

    https://doi.org/10.1016/j.triboint.2010.11.008

61. Suresha S, Sridhara BK, 2010a, Effect of addition of graphite particulates on the wear behaviour in aluminium-silicon carbide-graphite composites. *Mater Des*, 31: 1804–1812.

    https://doi.org/10.1016/j.matdes.2009.11.015

62. Kato H, Takama M, Iwai Y, *et al*., 2003, Wear and mechanical properties of sintered copper-tin composites containing graphite or molybdenum disulfide. *Wear*, 225: 573–578.

    https://doi.org/10.1016/S0043-1648(03)00072-3

63. Zhang Y, Epshteyn Y, Chromik RR, 2018, Dry sliding wear behaviour of cold-sprayed Cu-MoS_2 and Cu-MoS_2-WC composite coatings: The influence of WC. *Tribol Int*, 123: 296–306.

    https://doi.org/10.1016/j.triboint.2017.12.015

64. Tu J, Rong W, Guo S, *et al*., 2003, Dry sliding wear behavior of *in situ* Cu-TiB_2 nanocomposites against medium carbon steel. *Wear*, 255: 832–835.

    https://doi.org/10.1016/S0043-1648(03)00115-7

65. Valero ML, Corredor D, Camurri C, *et al*., 2005, Performance and characterization of dispersion strengthened Cu-TiB_2 composite for electrical use. *Mater Characterization*, 55: 252–262.

    https://doi.org/10.1016/j.matchar.2005.04.006

66. Kim JS, Kwon YS, Dudina DV, *et al*., 2005, Nanocomposites

TiB2-Cu: Consolidation and erosion behavior. *J Mater Sci*, 40: 3491–3495.

https://doi.org/10.1007/s10853-005-2854-2

67. Agarwal A, Dahotre NB, Sudarshan TS, 1999, Evolution of interface in pulsed electrode deposited titanium diboride on copper and steel. *Surf Eng*, 15: 27–32.

https://doi.org/10.1179/026708499322911601

68. Tu J, Wang NY, Yang YZ, *et al*., 2002, Preparation and properties of TiB_2 nanoparticle reinforced copper matrix composites by *in situ* processing. *Mater Lett*, 52: 448–452.

https://doi.org/10.1016/S0167-577X(01)00442-6

69. Munro RG, 2000, Material properties of titanium diboride. *J Res Natl Inst Stand Technol*, 105: 709.

https://doi.org/10.6028/jres.105.057

70. Kim JS, Kwon YS, Lomovsky OI, *et al*., 2007, Cold spraying of *in situ* produced TiB_2-Cu nanocomposite powders. *Comp Sci Technol*, 67: 2292–2296.

https://doi.org/10.1016/j.compscitech.2007.01.019

71. Calli C, Tazegul O, Kayali ES, 2017, Wear and corrosion characteristics of copper-based composite coatings. *Ind Lubr Tribol*, 69: 300–305.

https://doi.org/10.1108/ILT-07-2016-0146